Polymer 49 (2008) 3973–3978

Contents lists available at ScienceDirect

Polymer

journal homepage: www.elsevier.com/locate/polymer

Crystalline–crystalline poly(3-hexylthiophene)–polyethylene diblock copolymers: Solidification from the melt

Christian Müller [a], Christopher P. Radano [b,1], Paul Smith [a,c], Natalie Stingelin-Stutzmann [a,c,*]

[a] Department of Materials, ETH Zürich, CH-8093 Zürich, Switzerland
[b] Laboratory of Macromolecular and Organic Chemistry, Technische Universiteit Eindhoven, 5600 MB Eindhoven, The Netherlands
[c] Centre for Materials Research, Queen Mary University of London, London E1 4NS, UK

ARTICLE INFO

Article history:
Received 29 April 2008
Accepted 2 July 2008
Available online 12 July 2008

Keywords:
Crystalline–crystalline diblock copolymers
Organic semiconductors
Polythiophene

ABSTRACT

We report on the development of the solid-state structure from the melt of crystalline–crystalline diblock copolymers consisting of the semiconducting poly(3-hexylthiophene) (P3HT) and insulating polyethylene (PE) – a material combination that previously was shown to feature promising characteristics for applications in flexible organic electronics. The nature of the structures obtained from the melt was found to generally be dictated by crystallization of the PE block, which solidified *after* the P3HT sequence. This resulted in the formation of classical spherulitic structures for diblock copolymers of low P3HT content. At P3HT contents exceeding 10–20 wt%, the semiconductor block increasingly hampered crystallization of the PE moiety, with the P3HT entity arranging into columnar and at higher content into lamellar micelle-type domains. Unlike the rate of crystal growth of the two moieties, interestingly, the dimensionality of both entities of the diblock copolymers was found to be unaffected by the presence of the dissimilar block.

1. Introduction

In strong contrast to diblock copolymers that comprise one or two amorphous moieties, species consisting of two (semi-)*crystalline* parts belong to a relatively little explored class of polymeric materials. In fact, so far, such crystalline–crystalline systems have attracted attention mostly as compatibilizers for polymer blends, as thin layers for surface patterning and in selected biomedical applications [1–3]. This is surprising as their solid-state structure can be influenced by a number of factors in addition to those of materials comprising amorphous blocks (*i.e.* composition, miscibility, structure in the fluid phase, application of external force fields) [4–7] – most prominently, the sequence and kinetics of crystallization of the blocks. Thus, additional processing options can be accessed and a greater variety of solid-state structures – and therewith properties – be realized when compared to diblock copolymers containing at least one amorphous moiety.

Recently, we reported on the synthesis and solution-processing of crystalline–crystalline diblock copolymers comprising the semiconducting poly(3-hexylthiophene) and insulating polyethylene (P3HT–PE) [8,9]. The ultimate properties of films produced were principally dominated by the sequence of crystallization of the two moieties, which could be manipulated by the block copolymer composition, polymer solution concentration and casting conditions [9]. It was found that the solidification of the conjugated P3HT prior to the insulating PE was highly beneficial for inducing concomitant excellent electronic- and mechanical characteristics.

In the present study we focused on solidification and structure development of these diblock copolymers from the *melt*. We investigated phase separation, crystal nucleation, rate of growth, dimensionality and degree of crystallinity of the individual blocks of these intriguing materials.

2. Materials and methods

2.1. Materials

Synthesis and characterization of the diblock copolymers with poly(3-hexylthiophene)–polyethylene (P3HT–PE) weight ratios of 5–95, 10–90, 20–80 and 35–65, used in this work, were previously described [8]. The corresponding homopolymers, P3HT (regioregularity ~96%; $M_w = 22$ kg mol^{-1}, $M_n = 14$ kg mol^{-1}) and HDPE (Standard reference material 1484a; $M_w = 120$ kg mol^{-1}, $M_n = 101$ kg mol^{-1}), were supplied by, respectively, Merck Chemicals, UK, and the National Institute of Standards and Technology (NIST), USA. The antioxidant Irganox® 1010 (Ciba Special Chemicals,

* Corresponding author. Centre for Materials Research, Queen Mary University of London, London E1 4NS, UK. Tel.: +44 20 7882 7674; fax: +44 20 8981 9804.
E-mail address: n.stingelin-stutzmann@qmul.ac.uk (N. Stingelin-Stutzmann).
[1] Present address: Evonik RohMax USA, Inc., 723 Electronic Drive, Horsham, PA 19044-4050, USA.

0032-3861/$ – see front matter Crown Copyright © 2008 Published by Elsevier Ltd. All rights reserved.
doi:10.1016/j.polymer.2008.07.006

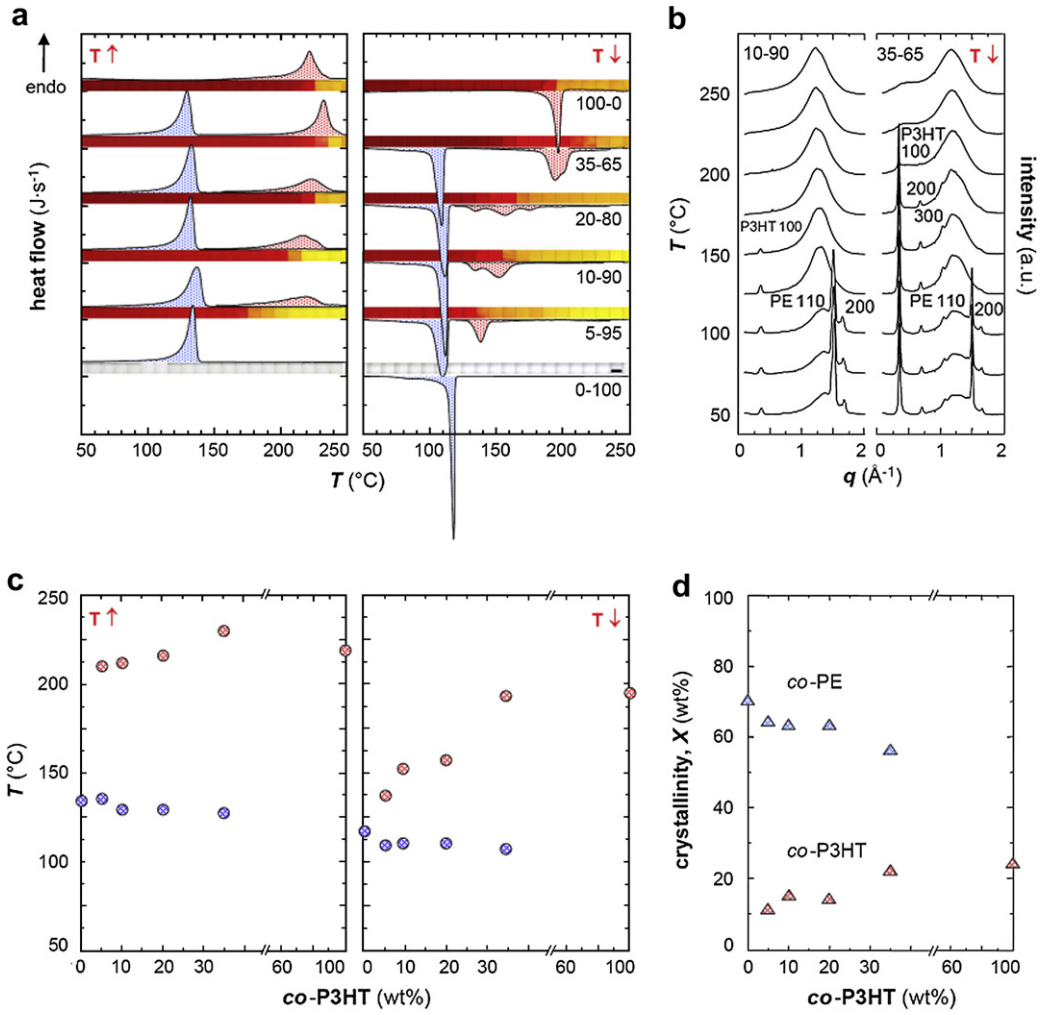

Fig. 1. (a) Differential scanning calorimetry (DSC) second heating and cooling thermograms (left and right panel, respectively) of P3HT–PE copolymers and corresponding homopolymers: blue- and red-shaded areas indicate thermal transitions of the PE and P3HT moieties, respectively (signal associated with the P3HT block is increased by factor 5). Corresponding unpolarized optical micrographs of thin polymer films are also shown, which display the distinct color change of the alkylthiophene block from red to yellow/orange during melting, and *vice versa* during solidification (scale-bar bottom-right 0.5 mm). (b) Wide-angle X-ray scattering (WAXS) diffractograms of 10–90 and 35–65 wt% P3HT–PE recorded during cooling from the melt. Note the exceptionally weak P3HT *h*00 diffraction in the case of 10–90 compared to *e.g.* the 35–65 diblock copolymer, suggesting a decrease in crystalline order of P3HT. (c) Non-equilibrium temperature-composition diagrams of P3HT–PE diblock copolymers constructed from peak temperatures in second heating (left) and cooling (right) DSC thermograms. (d) Degree of crystallinity, *X*, of the two copolymer blocks, *vs.* copolymer composition (PE moiety red; P3HT block blue) deduced from second DSC heating thermograms.

Switzerland) was added in a weight ratio of approximately 1:99 to all polymers.

2.2. Thin film preparation

Homogeneous solutions in xylene (Aldrich; used as-received) containing ~1 wt% of the various polymers were prepared at 125 °C, then cast onto glass slides, followed by evaporation of the solvent at ambient and subsequent melting at 250 °C, to produce thin films of ~50 μm thickness for optical microscopy analysis.

2.3. Thermal analysis

Differential scanning calorimetry (DSC) was conducted under nitrogen at a scan rate of 10 °C min^{-1} with a Mettler Toledo DSC822 instrument. The sample weight was ~5 mg. Isothermal crystallization was monitored after rapidly cooling samples at 50 °C min^{-1} from 250 °C to the desired temperature.

2.4. Optical microscopy

Transmission optical microscopy was carried out with a Leica DMRX polarizing microscope equipped with a Mettler Toledo FP82HT hot stage that was continuously flushed with nitrogen. Thin films of the various copolymers were heated to 250 °C and then cooled at a rate of 10 °C min^{-1}. Degradation at elevated temperatures was minimized by limiting exposure to light to the time required for image acquisition. Isothermal crystallization of the PE fraction was conducted at various temperatures after cooling the material at 20 °C min^{-1} from ~170 °C (at which all PE nuclei are thought to be destroyed [10]).

2.5. X-ray diffraction

Variable-temperature X-ray diffraction was carried out on polymer samples (sealed in aluminum pans and placed in a Linkham THMS600 hot stage) using synchrotron radiation ($\lambda = 1.240$ Å) at the Dutch-Belgian beamline (Dubble) of the European Synchrotron Radiation Facility (ESRF), Grenoble, France [11]. Samples were

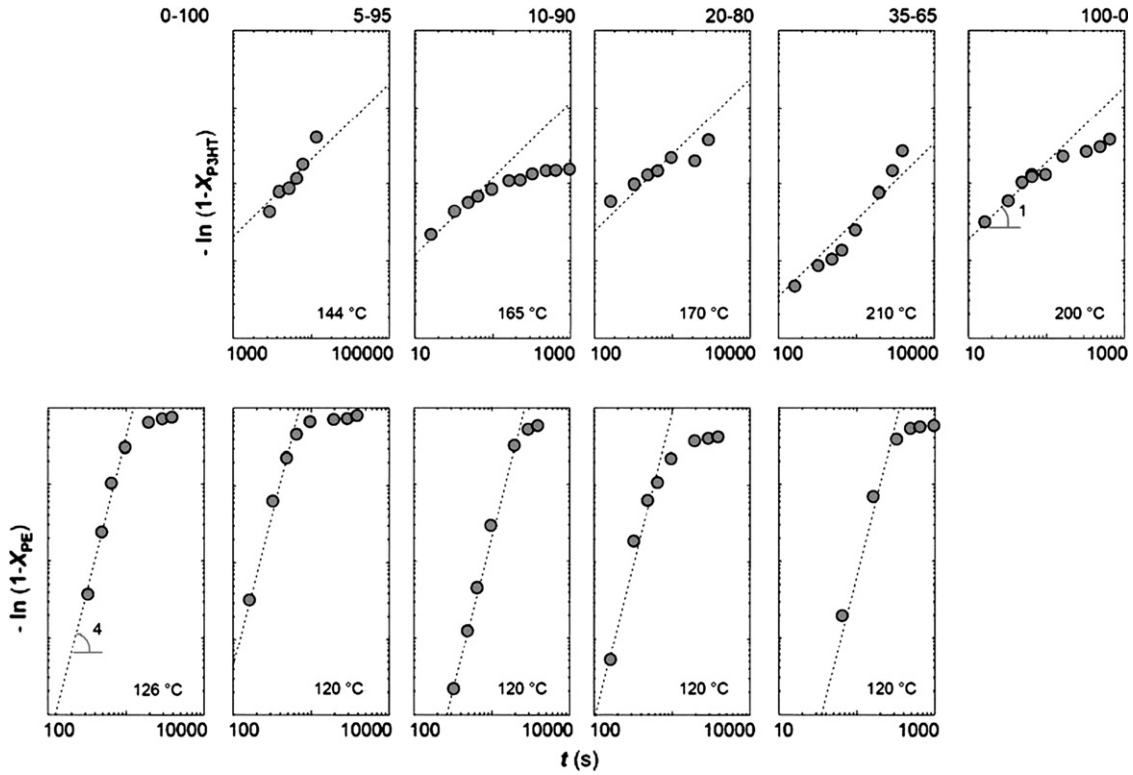

Fig. 2. Avrami plots for the P3HT moiety (top) and PE block (bottom). *X*(P3HT block) and *X*(PE block) were calculated from the enthalpies of fusion in DSC heating thermograms recorded immediately after isothermal crystallization for a period of time, *t*, at temperatures indicated. Avrami coefficients, *n*, of 1 and 4 for P3HT and PE, respectively, were deduced from the slope, as indicated [19].

cooled from 250 °C to ambient at a rate of 10 °C min^{-1}. Transmission wide-angle X-ray scattering (WAXS) patterns were recorded with a 2D-camera, accessing wavenumbers, *q*, between 0.1 and 2 Å^{-1}. A multi-wire gas-filled area detector placed at 8 m distance from the sample was utilized for the acquisition of small-angle X-ray scattering (SAXS) patterns within a *q* range of 0.05–0.85 nm^{-1}. The two-dimensional diffraction patterns were radially averaged after correction for background radiation and calibrated with high-density polyethylene (WAXS) and a wet rat-tail collagen standard (SAXS), respectively.

2.6. Crystallinity

The degree of crystallinity, *X*, of the diblock copolymer moieties, as well as of the two corresponding homopolymers, was calculated according to $X = \Delta H/\Delta H_0$, where ΔH is the enthalpy of fusion determined by integrating DSC endotherms normalized to the respective weight fractions and ΔH_0 is the enthalpy of fusion of 100% crystalline material, with ΔH_0 (PE) = 277 J g^{-1} and ΔH_0 (P3HT) = 99 J g^{-1} [12,13].

3. Results and discussion

3.1. Melting

The P3HT block in all diblock copolymers invariably exhibited higher melting and crystallization temperatures, respectively, T_m and T_c, than the PE moiety (Fig. 1a and b). The peak melting temperatures of either block were relatively little affected by the presence of the other entity (see Fig. 1c), which is indicative of limited miscibility in the melt, as was also observed for blends of the corresponding homopolymers [14]. Limited compatibility of the two fractions appeared to exist only at low P3HT contents (≤5 wt%) at elevated temperatures, as evident from the distinct color transition from red to orange/yellow – attributed to increased disorder of the P3HT block [15,16] – that occurred for the 5–95 block copolymer at temperatures slightly below that of the P3HT homopolymer and the P3HT-rich copolymers (cf. Fig. 1a).

3.2. Crystallization

In stark contrast to melting, crystallization of the individual blocks was significantly affected by the other entity. When cooled from the melt, both moieties exhibited lower crystallization temperatures than their respective homopolymers, with considerable super-cooling required for the P3HT moiety to solidify, especially for the 5–95, 10–90 and 20–80 block copolymers. Clearly, crystallization of both blocks was exceedingly hindered by the presence of the second moiety – a tendency also reported for several other crystalline–crystalline diblock copolymer systems [17,18]. As a consequence, in the solid-state, both polymer moieties featured a lower degree of crystallinity than the corresponding homopolymers subjected to a similar thermal history, as revealed by wide-angle X-ray scattering (WAXS) and differential scanning calorimetry (DSC) (cf. Fig. 1b and d).

3.3. Nucleation and dimensionality of crystal growth

In order to obtain insight into the dimensionality of crystal growth, isothermal crystallization experiments were conducted, and Avrami coefficients, *n*, were calculated according to the equation $(1 - X) = \exp(-k \cdot t^n)$. Here, *X* is the degree of crystallinity of the respective block developed at time *t* at a given temperature, and *k* and *n* are fitting parameters [19]. The Avrami coefficients were found to be unaffected for all copolymers when compared to those of the respective homopolymers, *i.e.* $n \sim 1$ for the P3HT-, and $n \sim 4$ for the PE-moiety (Fig. 2) [13,20]. This finding indicates that nucleation of the P3HT block was predetermined and crystallization

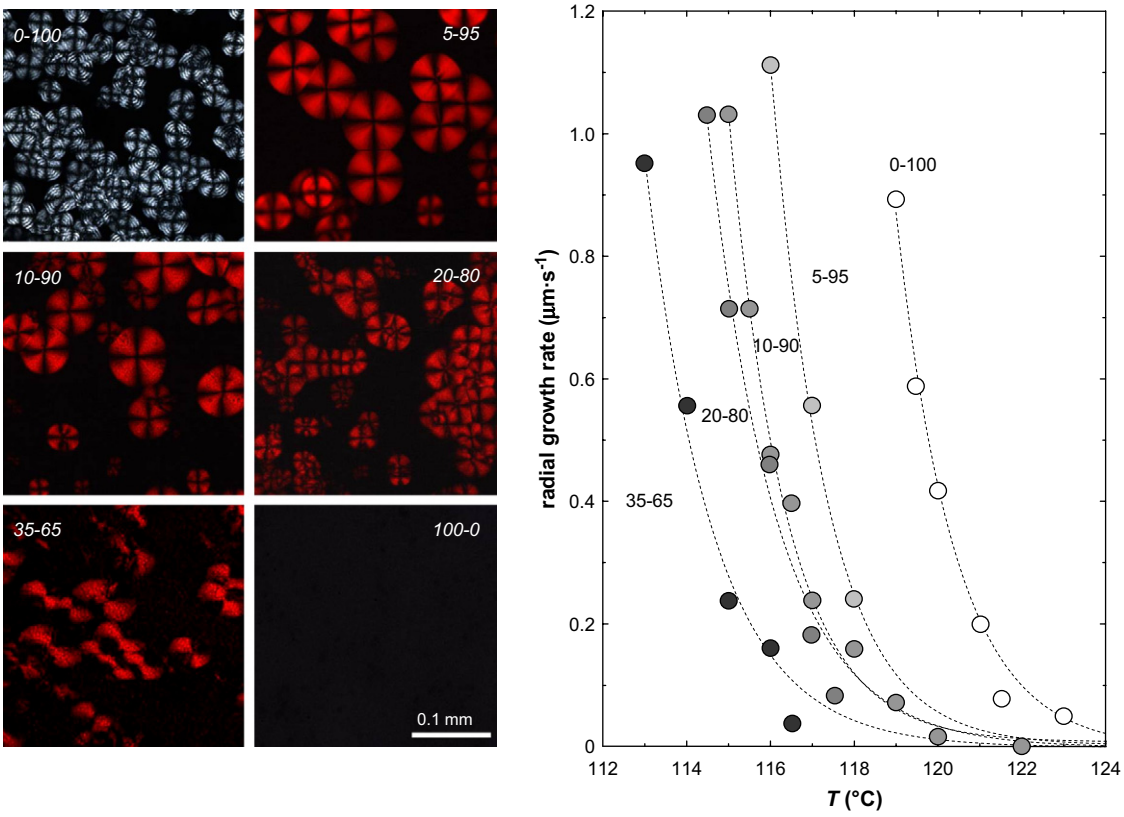

Fig. 3. Left panel: polarized optical micrographs of spherulitic entities after isothermal crystallization for 5 min for copolymers, and 2.5 min for 0–100 PE homopolymer, at temperatures corresponding to a linear growth rate of ~0.07 μm s^{-1} (0–100 ~122.5 °C, 5–95 ~120 °C, 10–90 and 20–80 ~118 °C, 35–65 ~117 °C). Images were taken at 125 °C to arrest further growth. Right panel: radial growth rate of spherulites as function of temperature, determined from spherulite radii after isothermal crystallization during different periods of time (dotted lines are drawn as a guide to the eye only).

occurred in a one-dimensional fashion, which is consistent with previous work that described structures of P3HT homopolymer and P3HT–PS diblock copolymer as "whiskers" [21,22]. The PE moiety, by contrast, nucleated sporadically and crystallized in a three-dimensional geometry, giving rise to the formation of the typical spherulitic super-structures displayed in a series of polarized optical micrographs, shown in Fig. 3. However, compared to the PE homopolymer solidified under comparable thermal conditions, a reduced number of nucleation centers, and, hence, spherulites, was observed.

3.4. Crystallization rate

The radial growth rate of spherulites that formed below T_c of PE was deduced from series of optical micrographs recorded at various times during isothermal crystallization at different temperatures (Fig. 3). As is evident from this set of data, spherulites developed more gradually for polymers that comprised an increasing amount of the P3HT moiety, indicating that the rate of crystallization of the PE block decreased.

Similarly, crystallization of the P3HT block was hampered by the presence of the PE moiety, resulting in a more gradual color change from yellow to dark red over a broader range of temperatures, as compared to the relatively rapid transition observed for the P3HT homopolymer (see Fig. 1).

3.5. Diblock copolymer domains

It is often observed for crystalline–crystalline diblock copolymer systems that the moiety that solidifies first largely dictates the ultimate solid structure, for instance poly(ε-caprolactone)–poly(ethylene glycol) (PCL–PEG), poly(L-lactide)–poly(ethylene glycol) (PLLA–PEG) and polyethylene–poly(ethylene oxide) (PE–PEO) [23–25]. Exceptions are, among others, polyethylene–poly(ε-caprolactone) (PE–PCL) and poly(L-lactide)–poly(ε-caprolactone) (PLLA–PCL), in which the PCL moieties rearrange the domains of the already solidified blocks (respectively, PE and PLLA), provided that the fraction of the PCL-block is sufficiently large [26,27].

P3HT–PE diblock copolymers of low P3HT content (*i.e.* 5–95 and 10–90) appear to belong to the latter class of species. As stated above, these copolymers formed well-developed spherulitic structures during solidification of the PE moiety, despite the fact that this block crystallized last (Fig. 3). By contrast, P3HT-rich copolymers (notably 35–65) featured more irregular spherulites, suggesting increased internal disorder because of more confined crystallization of PE.

In the molten state, the diblock copolymers – and most notably 20–80 and 35–65 – featured periodicities in SAXS patterns of, respectively, 0.1 and 0.08 nm^{-1}, corresponding to alternating P3HT- and PE-rich domains (cf. Fig. 4a).

Above and below the crystallization temperature of P3HT, but above T_c of PE, higher order SAXS periodicities could be discerned for 20–80 and 35–65 P3HT–PE. The latter featured characteristic ratios q_n/q_1 (q_1 being the first wavenumber), consistent with phase separation into hexagonal columnar ($q_n/q_1 = 1, \sqrt{3}, \sqrt{9}, \ldots$) and lamellar ($q_n/q_1 = 1, \sqrt{4}, \sqrt{9}, \ldots$) P3HT micelle-type entities, respectively (Fig. 4b, left) [28]. Note that the higher order reflections are broad, which suggests that the micellar domains are not well defined.

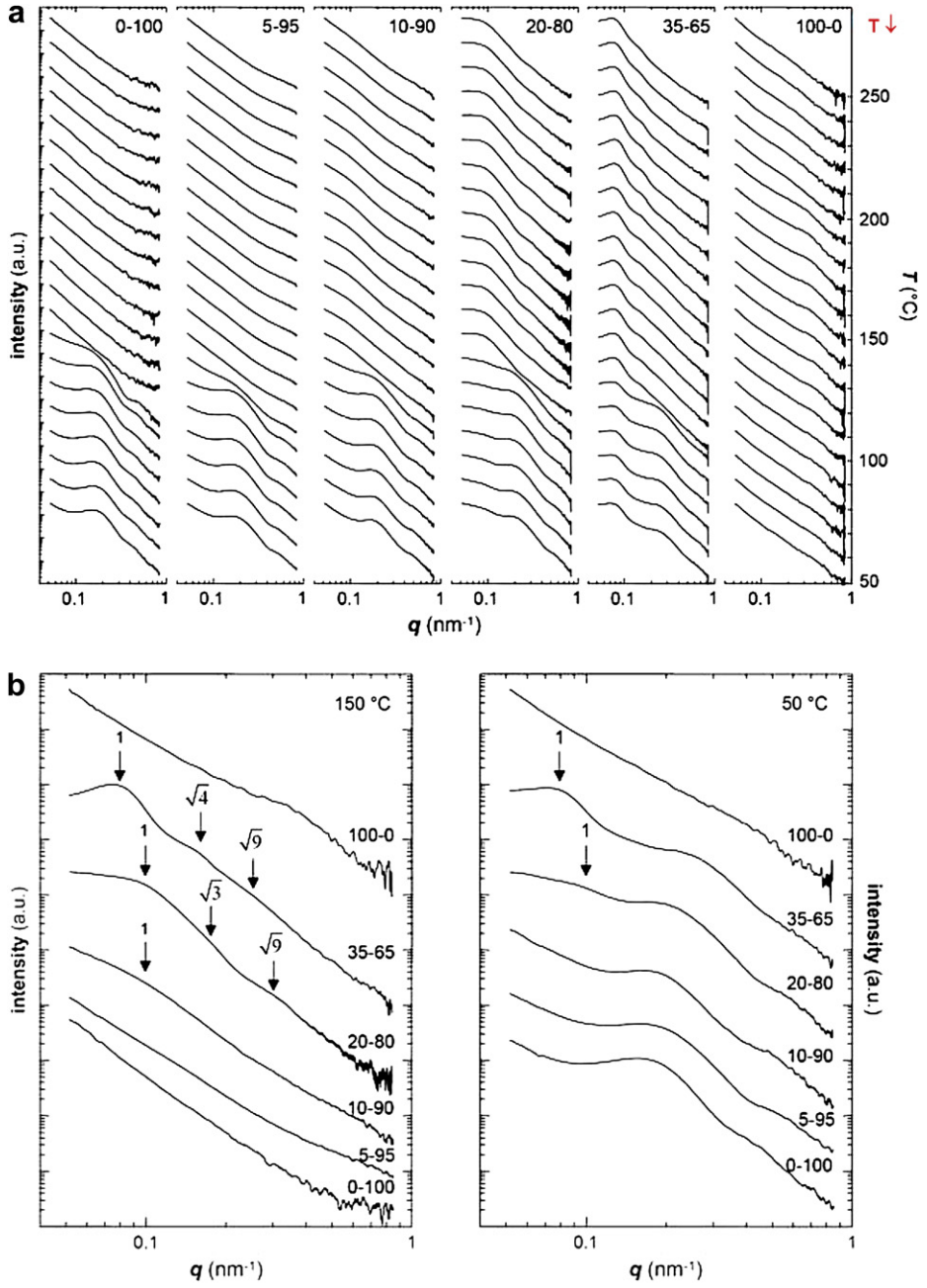

Fig. 4. Small-angle X-ray scattering (SAXS) patterns of P3HT–PE diblock of various compositions recorded during cooling from 250 °C to 50 °C, with higher order SAXS periodicities disconcernable only above T_c of the PE moiety (b).

Finally, in the fully solidified state, *i.e.* below T_c of PE, only those features associated with the PE lamellae, *i.e.* periodicities of around 0.2 nm^{-1}, persisted in the fully solidified copolymers. In addition, periodicities were recorded around 0.08–0.10 nm^{-1} (Fig. 4b, right), which are due to the classical lamellar features attributed to lamellar stacking of crystalline and amorphous domains [29,30], although the q values are lower than those observed in the corresponding homopolymers solidified under comparable experimental conditions [29–31].

The results presented here indicate that the solid-state structure of the novel crystalline–crystalline semi-conducting/insolating diblock copolymers consisted of (semi-)crystalline P3HT micellar-like entities dispersed in regions composed of amorphous/crystalline lamellar PE, which may explain the excellent electronic characteristics of these polymers when properly processed [9].

Acknowledgements

The authors are deeply indebted to Drs. W. Bras, K. Kvashnina and N. Vilayphiou for their hospitality and support at the Dutch-Belgium (Dubble) beamline of the European Synchrotron Radiation Facility (ESRF), Grenoble, France, where all WAXS and SAXS characterization was conducted. C.M. would like to thank Drs. K. Feldman, F. Choffat, M. Kristiansen, T. A. Tervoort, G. Beaucage and H. Goossens for fruitful discussions. We are grateful to Geordies' for providing a delightful environment, in which most of this manuscript was drafted. P.S. wishes to express his profound gratitude to the Engineering, Materials and Physics (*Emphysis*) Consortium of Queen Mary, University of London for their invitation to participate in their Prestige Visiting Researcher Programme, to The Leverhulme Trust for granting a Visiting Professorship at Queen Mary, University of London, during which time this project was completed; and

to his hosts Dr. Natalie Stingelin and Prof. Ton Peijs for their invaluable support.

References

[1] Wang Y, Hillmyer MA. J Polym Sci Part A Polym Chem 2001;39:2755–66.
[2] Ho RM, Hsieh PY, Tseng WH, Lin CC, Huang BH, Lotz B. Macromolecules 2003; 36:9085–92.
[3] Hamley IW, Castelletto V, Castillo RV, Müller AJ, Martin CM, Pollet E, et al. Macromolecules 2005;38:463–72.
[4] Bates FS, Fredrickson GH. Annu Rev Phys Chem 1990;41:525–57.
[5] Bates FS. Science 1991;251:898–905.
[6] Khandpur AK, Forster S, Bates FS, Hamley IW, Ryan AJ, Bras W, et al. Macromolecules 1995;28:8796–806.
[7] Park C, Yoon J, Thomas EL. Polymer 2003;44:6725–60.
[8] Radano CP, Scherman OA, Stingelin-Stutzmann N, Müller C, Breiby DW, Smith P, et al. J Am Chem Soc 2005;127:12502–3.
[9] Müller C, Goffri S, Andreasen JW, Breiby DW, Chanzy HD, Janssen RAJ, et al. Adv Funct Mater 2007;17:2674–9.
[10] Ergoz E, Fatou JG, Mandelkern L. Macromolecules 1972;5:147–57.
[11] Bras W. J Macromol Sci Phys 1998;37:557–65.
[12] Wunderlich B, Dole M. J Polym Sci 1957;24:201–13.
[13] Malik S, Nandi AK. J Polym Sci Part B Polym Phys 2002;40:2073–85.
[14] Goffri S, Müller C, Stingelin-Stutzmann N, Breiby DW, Radano CP, Andreasen JW, et al. Nat Mater 2006;5:950–6.
[15] Rughooputh SDDV, Hotta S, Heeger AJ, Wudl F. J Polym Sci Part B Polym Phys 1987;25:1071–8.
[16] Inganäs O, Salaneck WR, Österholm JE, Laakso J. Synth Met 1988;22: 395–406.
[17] Müller AJ, Albuerne J, Marquez L, Raquez JM, Degée P, Dubois P, et al. Faraday Discuss 2005;128:231–52.
[18] Müller AJ, Arnal ML, Balsamo V. Lect Notes Phys 2007;714:229–59.
[19] Avrami M. J Chem Phys 1939;7:1103–12.
[20] Rabesiaka J, Kovacs AJ. J Appl Phys 1961;32:2314–20.
[21] Ihn KJ, Moulton J, Smith P. J Polym Sci Part B Polym Phys 1993;31: 735–42.
[22] Liu J, Sheina E, Kowalewski T, McCullough RD. Angew Chem Int Ed 2002;41: 329–32.
[23] Bogdanov B, Vidts A, Schacht E, Berghmans H. Macromolecules 1999;32: 726–31.
[24] Sun J, Hong Z, Yang L, Tang Z, Chen X, Jing X. Polymer 2004;45:5969–77.
[25] Sun L, Liu Y, Zhu L, Hsiao BS, Avil-Orta CA. Polymer 2004;45:8181–93.
[26] Nojima S, Akutsu Y, Washino A, Tanimoto S. Polymer 2004;45:7317–24.
[27] Hamley IW, Parras P, Castelletto V, Castillo RV, Müller AJ, Pollet E, et al. Macromol Chem Phys 2006;207:941–53.
[28] Hamley IW. The physics of block copolymers. Oxford: Oxford University Press; 1998. p. 22ff.
[29] Mandelkern L, Posner AS, Diorio AF, Roberts DE. J Appl Phys 1961;32:1509–17.
[30] Fisher EW, Schmidt GF. Angew Chem 1962;74:551–62.
[31] Zhang R, Li B, Iovu MC, Jeffries-El M, Sauvé G, Cooper J, et al. J Am Chem Soc 2006;128:3480–1.